Laminar hydromagnetic natural convection flow along a heated vertical surface in a stratified environment with internal heat absorption

Ali J. Chamkha

Abstract: The problem of steady, laminar, natural convection flow along a vertical permeable surface immersed in a thermally stratified environment in the presence of magnetic-field and heat-absorption effects is studied numerically. Conditions for similarity solutions are determined for arbitrary stable and unstable thermal environment stratification. Numerical solution of the similarity equations is performed using an implicit, iterative, tri-diagonal finite-difference method. Comparison with previously published work is performed and the results are found to be in excellent agreement. The effects of Hartmann number, heat-absorption coefficient, and the wall mass-transfer parameter on the velocity and temperature profiles as well as the skin-friction coefficient and Nusselt number are presented graphically and discussed. It is found that both the magnetic-field and heat-absorption effects eliminate the occurrence of the fluid backflow and temperature deficit in the outer part of the boundary layer predicted for the nonmagnetic case.

PACS Nos.: 44.20, 44.25, 47.65

Résumé : Nous étudions numériquement l'écoulement convectif naturel, laminaire et stationnaire le long d'une surface verticale perméable plongée dans un environnement thermiquement stratifié, en présence d'un champ magnétique et avec absorption de chaleur. Nous déterminons les conditions pour les solutions de similarité dans les situations avec stratification stable et instable. Une méthode aux différences finies, itérative et tri-diagonale nous fournit une solution numérique des équations de similarité. Nous comparons avec des travaux déjà publiés et trouvons un excellent accord. Nous présentons graphiquement et analysons nos résultats pour les effets du nombre de Hartmann, du coefficient d'absorption thermique et du transfert de masse sur les profils de vitesse et de température, ainsi que sur le coefficient de friction à la surface et sur le nombre de Nusselt. Nous trouvons que le champ magnétique et les effets d'absorption de chaleur éliminent le flux de retour et le déficit en température dans la partie extérieure de la couche limite qui sont prédits pour le cas sans champ magnétique.

[Traduit par la Rédaction]

Received 8 August 2001. Accepted 12 December 2001. Published on the NRC Research Press Web site at `http://cjp.nrc.ca/` on 3 October 2002.

A.J. Chamkha. Department of Mechanical Engineering, Kuwait University, P.O. Box 5969, Safat, 13060 - Kuwait (e-mail: chamkha@kuc01.kuniv.edu.kw).

 DOI: 10.1139/P02-010

1. Introduction

Natural convection flows of electrically conducting and heat-generating or absorbing fluids in the presence of a transverse magnetic field have received considerable interest in recent years. This is because many industrial and engineering applications involve such flows. Examples of these applications include crystal growth, geothermal systems, heat exchangers, nuclear reactors, metallurgical processes, and others. In natural and some industrial free convection heat transfer processes, the density of the fluid is often stably stratified due to the presence of some dissolved species. In most practical situations, the concentration of these species is considered to be dilute. The condition of stable thermal stratification is realized when the fluid temperature increases with height in a gravitational field with the exception of water between 0°C and 4°C as mentioned by Angirasa and Srinivasan [1].

Understanding of processes involving thermal ambient stratification in the presence of heat generation or absorption and magnetic-field effects requires the solution of the Navier–Stokes equations. These equations can be simplified when the boundary-layer theory is assumed. With the use of special transformations, the boundary-layer partial differential equations can reduce to a set of ordinary differential equations (similarity equations) that can be solved numerically with minimum effort. In many situations, these self-similar solutions are very useful, as they predict the physical characteristics of the problem correctly. The search for similarity equations started a long time ago and has continued in recent years. Ostrach [2] reported an analysis of laminar free convection flow and heat transfer about an isothermal flat plate based on the numerical solution of similarity equations. Sparrow and Gregg [3] reported similar solutions for free convection from a non-isothermal vertical plate. Cheesewright [4] and Yang et al. [5] considered natural convection flow from isothermal and non-isothermal plates immersed in a thermally stratified environment. Chen and Eichhorn [6,7] reported numerical and experimental solutions for natural convection flow over vertical surfaces and simple bodies immersed in a thermally stratified fluid. Semenov [8] developed similarity solutions for all possible distributions of wall and environment temperatures. Merkin [9] found that a singular behaviour is predicted for the case of non-isothermal surface with fixed environment temperature when a critical value of the wall temperature parameter is exceeded. Kulkarni et al. [10] claimed to have found a new class of similarity solutions for natural convection flow over an isothermal vertical wall in a thermally stratified medium. Later, Henkes and Hoogendoorn [11] reported a more general new class of similar solutions for laminar natural convection boundary-layer flow along a heated vertical plate in a stratified environment. Also, Henkes and Hoogendoorn [11] showed that the similar solutions reported earlier by Semenov [8] were more general than those reported by Kulkarni et al. [10]. Some other related works on thermal stratification can be found in the papers by Eichhorn [12], Eichhorn et al. [13], Venkatachala and Nath [14], Angirasa and Srinivasan [15] and Angirasa and Peterson [16].

The objective of this work is to report the conditions for similarity solutions for steady, laminar, natural convection flow along a non-isothermal vertical surface immersed in a thermally stratified environment in the presence of a transverse non-uniform magnetic field, heat generation or absorption, and surface mass transfer. This work is based on the transformations reported earlier by Henkes and Hoogendoorn [11].

2. Governing equations

Consider steady, laminar, natural convection boundary-layer flow along a permeable heated vertical surface in a stratified environment in the presence of a transverse magnetic field and internal heat generation or absorption. Let x be the distance along the plate (vertical coordinate) and y be the distance normal to the plate. Both the magnetic field and the internal heat generation/absorption are assumed to vary with x. Experimentally, the majority of flows of electrically conducting fluids occur in quite non-uniform magnetic fields. As mentioned by Branover [17], this is primarily due to the limited size of the magnet system, there being regions near the edges of the magnet poles where the magnetic-field

induction is not uniformly distributed. In addition, owing to manufacturing considerations, the magnet poles are frequently not continuous or not parallel or they may be smaller than the fluid flow regions. The variation of the magnetic-field induction along the surface can be accomplished by varying the width of the magnet gap on the surface in steps. The magnetic Reynolds number is assumed to be small so that the induced magnetic field can be neglected. Also, no electric field is assumed to exist (short circuit), and viscous dissipation, Joule heating, and the Hall effect are neglected. The fluid properties are assumed to be constant except the density in the thermal buoyancy term of the governing equations. These equations are based on the boundary-layer form of the balance laws of mass, linear momentum, and energy. Taking into consideration the Boussinesq approximation, these equations can be written as

$$\frac{\partial u}{\partial x} + \frac{\partial v}{\partial y} = 0 \tag{1}$$

$$u\frac{\partial u}{\partial x} + v\frac{\partial u}{\partial y} = \nu\frac{\partial^2 u}{\partial y^2} + g^*\beta[T - T_\infty(x)] - \frac{\sigma B^2(x)}{\rho}u \tag{2}$$

$$u\frac{\partial T}{\partial x} + v\frac{\partial T}{\partial y} = \frac{\nu}{\mathrm{Pr}}\frac{\partial^2 T}{\partial y^2} + \frac{Q(x)}{\rho c_\mathrm{p}}[T - T_\infty(x)] \tag{3}$$

where the various parameters are defined in the List of symbols section.

The boundary conditions for this problem are given by

$$\begin{aligned} &x = 0 : u \text{ and } T \text{ profiles specified} \\ &y = 0 : u = 0, \qquad v = -v_\mathrm{w}(x), \qquad T = T_\mathrm{w}(x) \\ &y \to \infty : u = 0, \qquad T = T_\infty(x) \end{aligned} \tag{4}$$

where $v_\mathrm{w}(x)$, $T_\mathrm{w}(x)$, and $T_\infty(x)$ are the wall mass transfer, wall temperature, and the fluid ambient or environment temperature.

Similarity equations for this problem are possible for special distributions of $B(x)$, $Q(x)$, $v_\mathrm{w}(x)$, $T_\mathrm{w}(x)$, and $T_\infty(x)$. Semenov [8] and later Henkes and Hoogendoorn [11] have given the distributions for $T_\mathrm{w}(x)$ and $T_\infty(x)$ and rewritten the temperature as follows:

$$\begin{aligned} &T_\mathrm{w}(x) = (m+1)\Delta T\xi^n + T_\mathrm{c}, T_\infty(x) = m\Delta T\xi^n + T_\mathrm{c} \\ &T = [m + g(\eta)]\Delta T\xi^n + T_\mathrm{c} \end{aligned} \tag{5}$$

where T_c is a constant and the transformed coordinates ξ and η and the characteristic temperature difference ΔT are given by

$$\begin{aligned} &\xi = Mx + N(\xi \geqslant 0) \\ &\eta = \left[\frac{g^*\beta\Delta T}{\nu^2}|M|\right]^{1/4}(Mx+N)^{(n-1)/4}y \\ &\Delta T = T_\mathrm{w} - T_\infty(0) \end{aligned} \tag{6}$$

The parameters m, n, M, and N are constants and $T_\infty(0)$ is the environment temperature at the leading edge of the surface.

Defining the stream function in the usual way as

$$u = \frac{\partial\psi}{\partial y}, \quad v = \frac{-\partial\psi}{\partial x} \tag{7}$$

and introducing the following transformation:

$$\psi = \left[\frac{g^*\beta\Delta T\nu^2}{|M|^3}\right]^{1/4} \xi^{(n+3)/4} f(\eta) \tag{8}$$

we obtain

$$u = \left[\frac{g^*\beta\Delta T\nu^2}{|M|^3}\right]^{1/2} \xi^{(n+1)/2} f'(\eta)$$

$$v = -\left[\frac{g^*\beta\Delta T\nu^2}{|M|^3}\right]^{1/4} M\xi^{(n-1)/4}\left[\left(\frac{n+3}{4}\right)f + \left(\frac{n-1}{4}\right)\eta f'\right] \tag{9}$$

Substituting (5), (6), and (9) into (1) to (4) and assuming that $B(x) = B_0(Mx+N)^{(n-1)/4}$, $Q(x) = Q_0(Mx+N)^{(n-1)/2}$, and $v_w(x) = v_0(Mx+N)^{(n-1)/4}$ (where B_0, Q_0, and v_0 are constants) results in the following similarity equations and boundary conditions:

$$f''' + \mathrm{sgn}(M)\left[\left(\frac{n+3}{4}\right) f\, f'' - \left(\frac{n+1}{2}\right) f'^2\right] + g - \mathrm{Ha}^2 f' = 0 \tag{10}$$

$$g'' + \mathrm{Pr}\ \mathrm{sgn}(M)\left[\left(\frac{n+3}{4}\right) f g' - n(g+m) f'\right] + \mathrm{Pr}\ \alpha g = 0 \tag{11}$$

$$\eta = 0: \quad f = f_0, \quad f' = 0, \quad g = 1$$
$$\eta \to \infty: \quad f' \to 0, \quad g \to 0 \tag{12}$$

where

$$\mathrm{Ha}^2 = \frac{\sigma B_0^2}{\rho(g^*\beta\Delta T|M|)^{1/2}}, \quad \alpha = \frac{Q_0}{\rho\, c_p(g^*\beta\Delta T\,|M|)^{1/2}}, \quad f_0 = \frac{v_0}{\left[\frac{g^*\beta\Delta T\nu^2}{|M|^3}\right]^{1/4} M(\frac{n+3}{4})} \tag{13}$$

are the square of the Hartmann number, dimensionless heat generation ($\alpha > 0$) or absorption ($\alpha < 0$) parameter, and dimensionless wall mass transfer parameter, respectively.

Equations (10) to (12) have the property that they contain various special cases. For instance, when $m = 0$, the case of nonstratified environment is recovered. Also, the case with constant wall temperature is obtained when $m = -1$. If all the parameters f_0, Ha, and Δ are equal to zero, the equations of Henkes and Hoogendoorn [11] are recovered.

Various limiting solutions of (10) to (12) with $f_0 = \mathrm{Ha} = \alpha = 0$ have been reported. Ostrach [2] considered the case of an isothermal surface with a nonstratified environment ($m = 0$, $\mathrm{sgn}(M) = 1$, and $n = 0$). Sparrow and Gregg [3] studied the case of a non-isothermal surface with a nonstratified environment ($m = 0$, $\mathrm{sgn}(M) = 1$, limited range of n values). The problem of Sparrow and Gregg [3] was extended to a stratified environment ($m = -1$, $\mathrm{sgn}(M) = 1$, limited range of n values) by Cheesewright [4], Yang et al. [5], and Merkin [9] (whole range of n values). Henkes and Hoogendoorn [11] reported solutions for the general case of negative M values for a non-isothermal surface with a stratified environment ($m = -1$, whole range of n values).

The skin-friction coefficient and the Nusselt number are important physical parameters for this flow and heat transfer situation. They can be defined in dimensionless form as follows:

$$C_f = \xi^{-(1+3n)/4} C_f^* = f''(0) \tag{14a}$$

$$\mathrm{Nu} = \xi^{(1-5n)/4}\mathrm{Nu}^* = -g'(0) \tag{14b}$$

where

$$C_f^* = \frac{\mu\,(\partial u/\partial y)_{y=0}}{\mu\,[(g^*\beta\,\Delta T)^3/(\nu^2|M|)]^{1/4}} \tag{15}$$

and

$$\mathrm{Nu}^* = \frac{k\,(\partial T/\partial y)_{y=0}}{k\,[g^*\beta\,\Delta T^5|M|\,/\,\nu^2]^{1/4}} \tag{16}$$

(μ and k are the fluid dynamic viscosity and thermal conductivity, respectively.)

3. Numerical method

Equations (10) and (11) are obviously nonlinear, coupled, ordinary differential equations that possess no closed-form solution. Therefore, they must be solved numerically, subject to the boundary conditions given by (12). The implicit, iterative finite-difference method discussed by Blottner [18] has proven to be adequate for the solutions of this type of equations. For this reason, this method is employed in the present work.

The method is implemented as follows: First, a change of variable is used in (10) such that $V = f'$. The resulting equation in V along with (11) are then expressed in the following general form:

$$\pi_1 F'' + \pi_2 F' + \pi_3 F + \pi_4 = 0 \tag{17}$$

where F is a typical dependent variable that stands for V or g and the π's are (in general) functions of the dependent and independent variables. At each iteration step, linearization of the equations takes place by evaluating the π's at the previous iteration. Then, all the equations in the form of (17) are discretized using three-point central difference quotients. This converts the differential equations into linear sets of algebraic equations that can be readily solved by the well-known Thomas algorithm (see Blottner [18]). With the solution for V known, the equation $f' - V = 0$ is then discretized and solved subject to the appropriate boundary condition by the trapezoidal rule. The computational domain in the η direction was made up of 196 non-uniform grid points. It is expected that most changes in the dependent variables occur in the region close to the surface where viscous effects dominate. However, small changes in the dependent variables are expected far away from the surface. For these reasons, variable step sizes in the η direction are employed. The initial step size $\Delta\eta_1$ and the growth factor K^* employed such that $\Delta\eta_{i+1} = K^*\Delta\eta_i$ (where the subscript i indicates the grid location) were 10^{-3} and 1.03, respectively. These values were found (by performing many numerical experimentations) to give accurate and grid-independent solutions. The solution convergence criterion employed in the present work was based on the difference between the values of the dependent variables at the current and the previous iterations. When this difference reached 10^{-5}, the solution was assumed converged and the iteration process was terminated.

To check or validate the correctness of the above numerical procedure, a direct comparison with the previously published work of Henkes and Hoogendoorn [11] on special cases of the problem under investigation is performed. As will be shown subsequently in Figs. 9 and 10, excellent agreement between the results is obtained. No comparison with experimental data for the general problem is possible because of the absence of such data at present as far as the authors are aware.

4. Results and discussion

In this section, a representative set of numerical results illustrating the influence of the Hartmann number Ha, the heat generation or absorption coefficient α, and the mass transfer parameter f_0 on the velocity and temperature profiles for a fixed wall temperature is shown. It should be mentioned that

Fig. 1. Effects of Ha on velocity profiles.

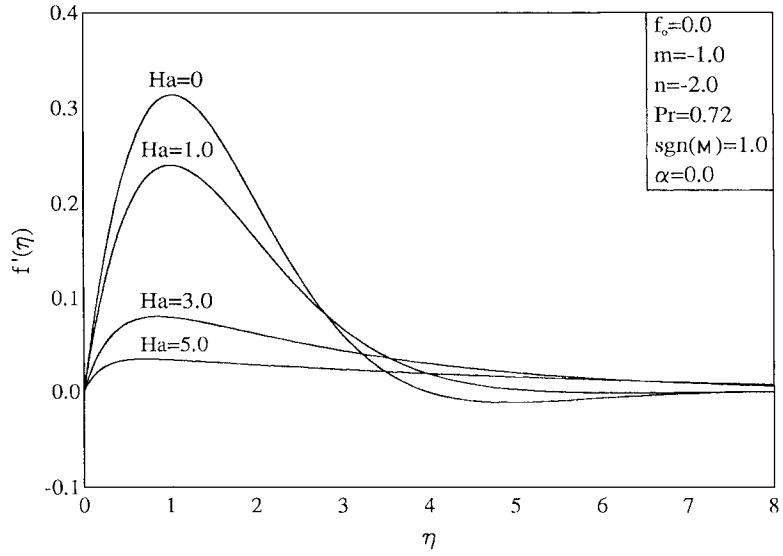

Fig. 2. Effects of Ha on temperature profiles.

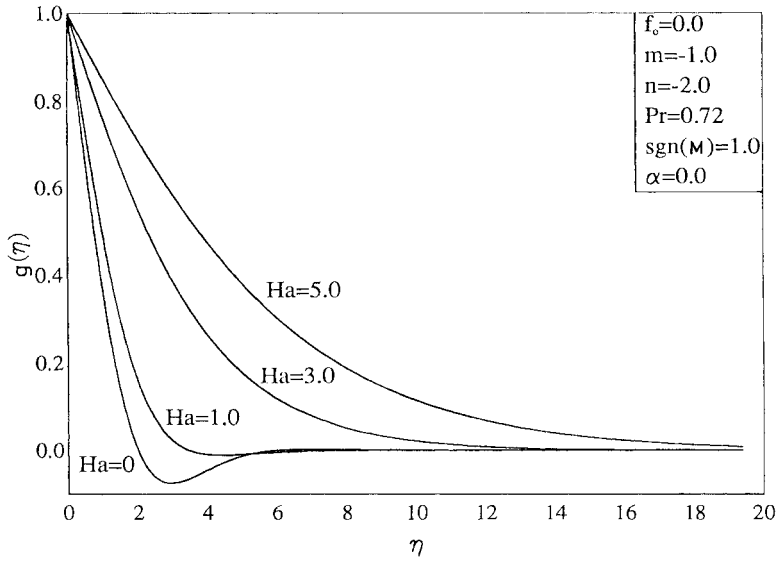

only negative values of α (heat absorption) will be considered because only these values can produce a qualitatively different behaviour for the flow and heat transfer situation considered in the present work. Figures 1 and 2 illustrate the influence of the magnetic Hartmann number Ha on the velocity and temperature profiles, respectively. Application of a transverse magnetic field normal to the flow direction gives rise to the magnetic Lorentz force that acts in the opposite direction of flow causing its velocity to decrease and its temperature to increase. In addition, the thermal boundary layer tends to increase as Ha increases. These behaviours are clearly depicted in Figs. 1 and 2. In the absence of the magnetic field (Ha = 0), it was reported by Henkes and Hoogendoorn [11] that for the parametric conditions of Figs. 1 and 2 (stably stratified environment), a backflow situation is predicted to occur far from the wall, while the fluid temperature close to the wall is predicted to be lower than that of the wall. It is clearly

Fig. 3. Effects of α on velocity profiles.

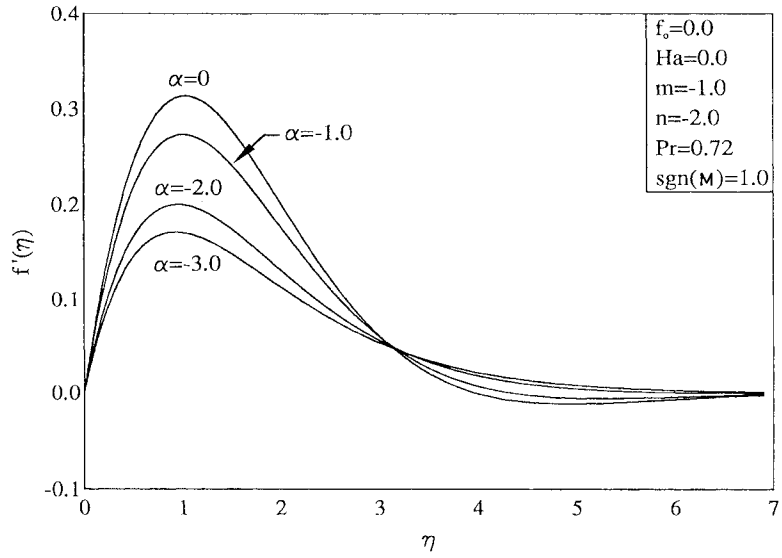

Fig. 4. Effects of α on temperature profiles.

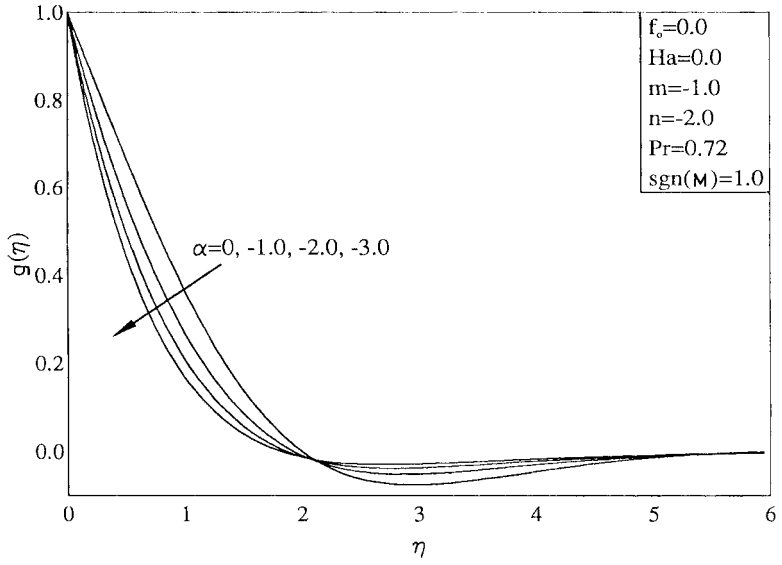

seen from Figs. 1 and 2 that, for a sufficiently strong magnetic field (large Hartmann number), these phenomena are prevented from happening. Figures 3 and 4 display the effects of heat absorption ($\alpha < 0$) on the velocity and temperature profiles for a situation of stably stratified environment, respectively. Heat absorption has the tendency to reduce the temperature distribution of the fluid along the surface. This causes the buoyancy force to decrease resulting in less flow along the surface. These behaviours are depicted by the decreases in both f' and g as $|\alpha|$ increases. It is interesting to observe that the small backflow and temperature deficit in the outer part of the boundary layer mentioned above are eliminated by increases in the heat-absorption effect. The effects of fluid wall mass transfer (suction or injection) on the velocity and temperature profiles for the flow situation considered in the previous figures are presented in Figs. 5 and 6, respectively. Imposition of fluid wall suction ($f_0 > 0$) has

Fig. 5. Effects of f_0 on velocity profiles.

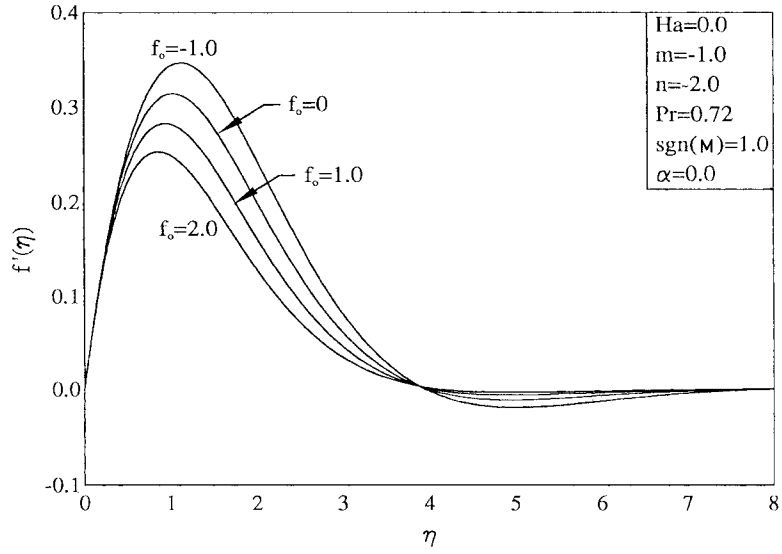

Fig. 6. Effects of f_0 on temperature profiles.

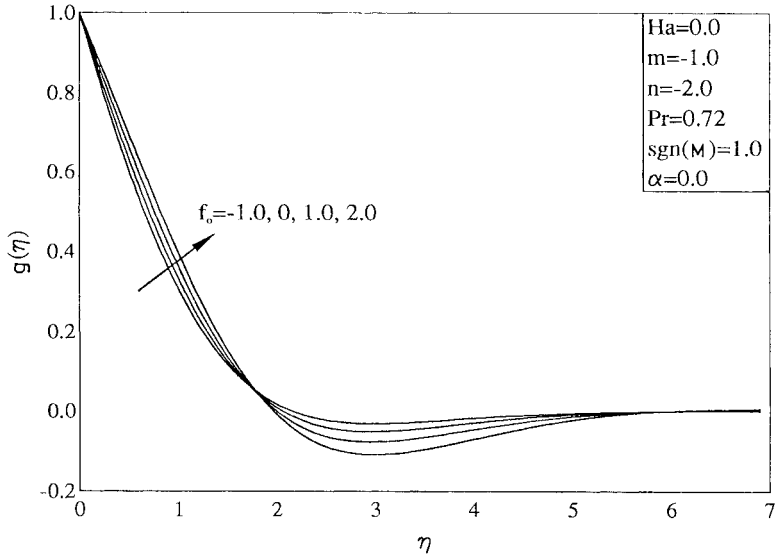

the effect of reducing the fluid velocity and increasing its temperature slightly in the region close to the wall. However, in the outer part of the boundary layer, the velocity tends to increase, causing the backflow there to diminish. In addition, the temperature deficit tends to increase in the outer part of the boundary layer as the suction effect increases. On the other hand, imposition of fluid wall injection ($f_0 < 0$) has the opposite effect on the velocity and temperature profiles, namely, increases in the velocity and reductions in the temperature close to the wall. The backflow condition discussed earlier tends to increase while the temperature deficit diminishes as the injection velocity increases. All of the above behaviours are clearly shown in Figs. 5 and 6. Figures 7 and 8 present the effects of the exponent of the wall and (or) environment temperature n on the velocity and temperature distributions in the presence of a moderate magnetic field (Ha = 1.0) for stably ($n < 0$) and unstably ($n > 0$) stratified environments, respectively. It is clearly observed that, in general, the flow velocity increases while the

Fig. 7. Effects of n on velocity profiles.

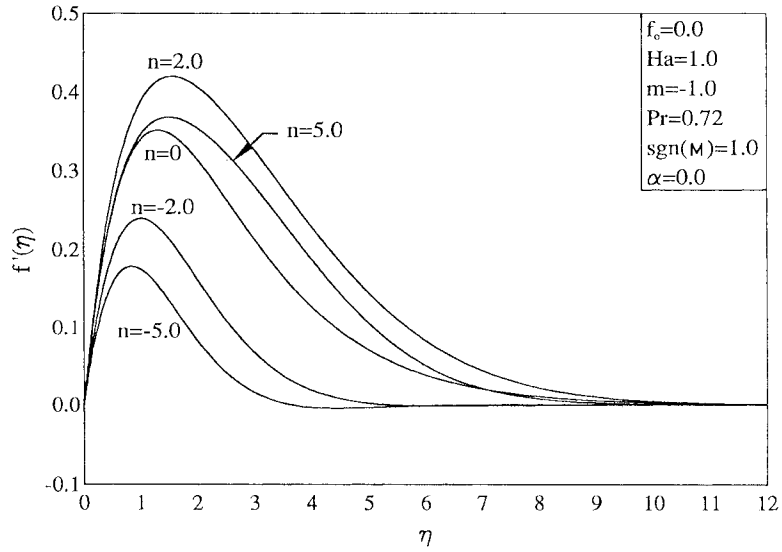

Fig. 8. Effects of n on temperature profiles.

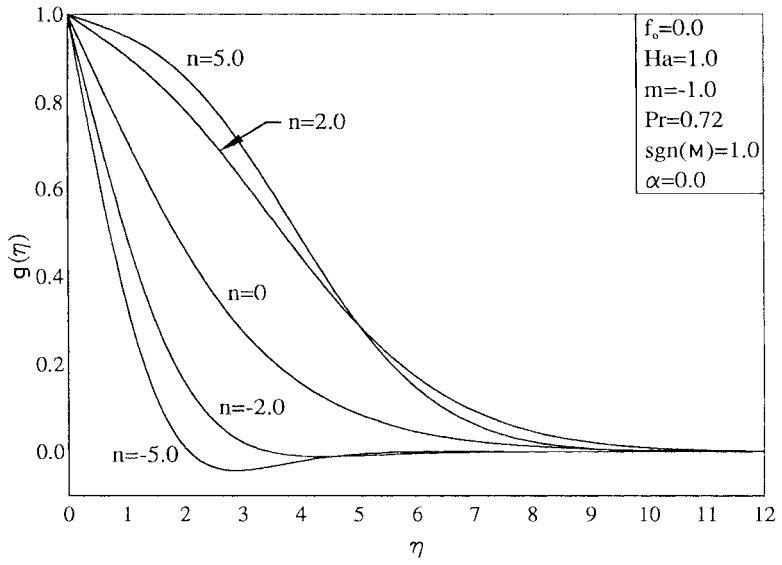

temperature decreases as the exponent n increases. It is obvious from Fig. 7 that for all the values of n used, no backflow condition exists. Also, there appears to be a critical value of $n > 0$ beyond which the velocity tends to decrease. This will be seen from Fig. 9. In Fig. 8, it is clear that no temperature deficit exists for the unstably stratified environment conditions ($n > 0$) employed. However, for the large stably stratified environment condition ($n = -5$), a temperature deficit exists even in the presence of a moderate magnetic field (Ha = 1.0). It can be deduced that a stronger magnetic field (Ha > 1.0) is required to eliminate this temperature deficit. Figures 9 and 10 depict the variations of the skin-friction coefficient C_f and the Nusselt number Nu for various parametric conditions, respectively. The reference curves in these figures correspond to the parametric values in the boxes appearing in these figures. First, it is seen that in the whole range of stably and unstably stratified environments ($-5 \leqslant n \leqslant 5$), the

Fig. 9. Variations of skin-friction coefficient for various parametric conditions.

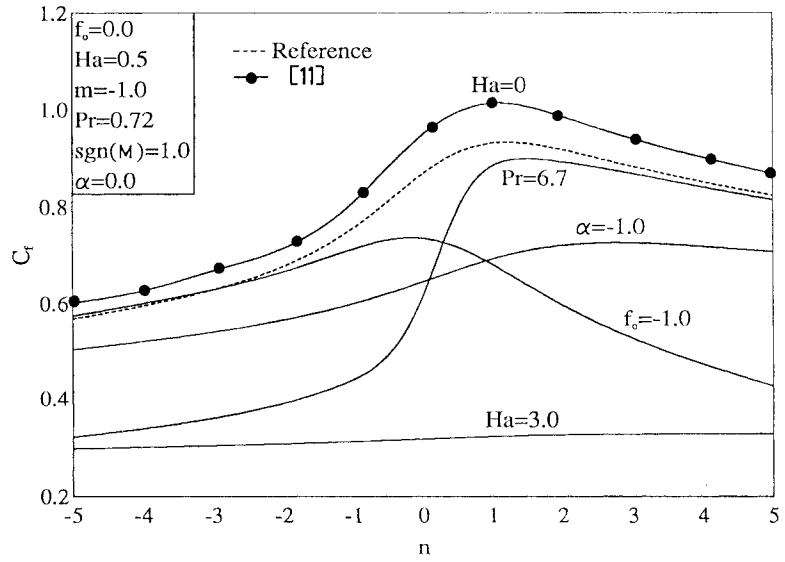

Fig. 10. Variations of Nusselt number for various parametric conditions.

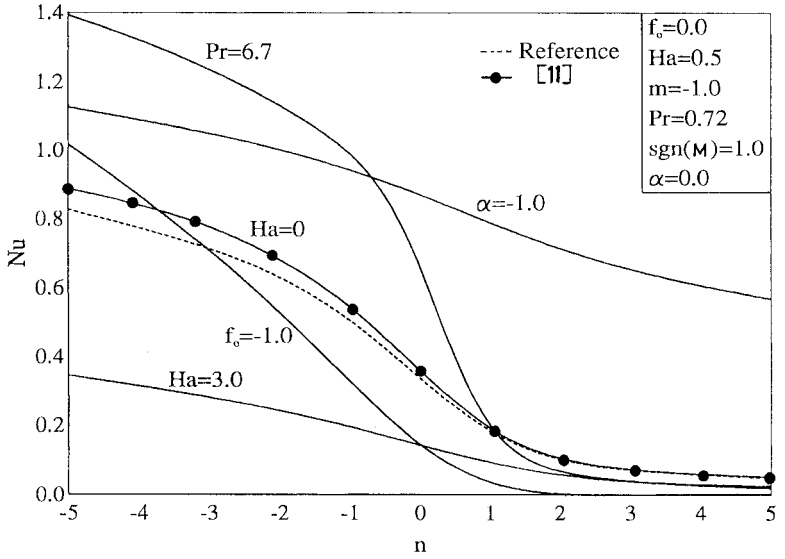

skin-friction coefficient increases to a maximum occurring in the vicinity of $n = 1.0$ and then decreases as n increases beyond this value. This suggests that the fluid velocity along the surface for the reference case increases as n increases until it reaches $n \cong 1.0$ beyond which the velocity starts to decrease. This phenomenon was seen for Ha = 1.0 in Fig. 7. The Nusselt number Nu tends to decrease gradually with n reaching an asymptotic value in the range $n > 0$. By looking at the curves associated with Ha = 0 and Ha = 3.0 in comparison with the reference curve, it can be concluded that both the skin-friction coefficient and the Nusselt number decrease due to the presence of the magnetic field for the whole range of n considered. The effects of Ha on C_f and Nu appear to be more pronounced in the range $(-5 \leqslant n < 0)$ than in the range $(0 \leqslant n \leqslant 5)$. In addition, inspection of the curves associated with $\alpha = -1.0$ in comparison with the reference curve shows that heat absorption reduces the skin-friction

coefficient while it increases the Nusselt number. Considering the curve corresponding to $f_0 = -1.0$, it is obvious that decreasing the mass transfer parameter decreases the values of both C_f and Nu in the range $(-3 \leqslant n \leqslant 5)$ whereas it increases them in the range $(-5 \leqslant n < -3)$. The effect of reducing f_0 appears to be more pronounced for unstably stratified environments ($n > 0$) than for stably stratified environments ($n < 0$). Finally, the effect of increasing the fluid Prandtl number Pr on the values of C_f and Nu in comparison with the reference curve is seen to reduce C_f in the whole n-range considered, to increase Nu in the range $(-5 \leqslant n \leqslant 1)$, and to decrease Nu in the range $(1 < n \leqslant 5)$. The influence of increasing the value of Pr is seen to be more pronounced in the stably stratified environment range $n < 0$.

5. Conclusion

The problem of steady, laminar, natural convection flow along a heated vertical surface in stably and unstably stratified environments in the presence of magnetic-field, heat-absorption, and wall mass-transfer effects was considered. The governing equations for this problem were developed, nondimensionalized, and transformed into a similarity form. The distributions of the magnetic-field strength, heat absorption, and wall mass transfer for various environment stratification situations necessary for similarity solutions were determined. Numerical solutions of the similarity equations were obtained by using an implicit, iterative, tri-diagonal, finite-difference method. A representative set of graphical results was presented and discussed. It was found that, for a fixed wall temperature, application of a transverse magnetic field or inclusion of heat-absorption effects eliminated the backflow and temperature deficit in the outer part of the boundary layer inherent in the nonmagnetic case. However, while the imposition of wall fluid suction eliminated the backflow condition, it increased the temperature deficit. Fluid wall injection produced the exact opposite behaviour. In addition, increasing the magnetic-field strength decreased both the skin-friction coefficient and the Nusselt number for both stably and unstably stratified environments. While heat absorption produced lower skin-friction coefficients, it increased the Nusselt number. The effect of fluid wall injection was predicted to decrease both the skin-friction coefficient and the Nusselt number for all considered unstable and some stable stratified environments.

References

1. D. Angirasa and J. Srinivasan. ASME J. Heat Transfer, **114**, 917 (1992).
2. S. Ostrach. NACA Report 1111. 1953.
3. E.M. Sparrow and J.L. Gregg. Trans. ASME, **80**, 379 (1958).
4. R. Cheesewright. Int. J. Heat Mass Transfer, **10**, 1847 (1967).
5. K.T. Yang, J.L. Novotny, and Y.S. Cheng. Int. J. Heat Mass Transfer, **15**, 1097 (1972).
6. C.C. Chen and R. Eichhorn. J. Heat Transfer, **98**, 446 (1976).
7. C.C. Chen and R. Eichhorn. Report No. UKY TR105-ME14-77. ORES Publications, College of Engineering, University of Kentucky, Lexington, Ky. 1977.
8. V.I. Semenov. Heat Transfer-Sov. Res. **16**, 69 (1984).
9. J.H. Merkin. J. Eng. Math. **19**, 189 (1985).
10. A.K. Kulkarni, H.R. Jacobs, and J.J. Hwang. Int. J. Heat Mass Transfer, **30**, 691 (1987).
11. R.A.W.M. Henkes and C.J. Hoogendoorn. Int. J. Heat Mass Transfer, **32**, 147 (1989).
12. R. Eichhorn. Prog. Heat Mass Transfer, **2**, 41 (1969).
13. R. Eichhorn, J.H. Leinhard, and C.C. Chen. Proc. 5th Int. Heat Transfer Conf., Tokyo, Japan. NC 1.3, 10. 1974.
14. B.J. Venkatachala and G. Nath. Int. J. Heat Mass Transfer, **24**, 1848 (1981).
15. D. Angirasa and J. Srinivasan. ASME J. Heat Transfer, **111**, 657 (1989).
16. D. Angirasa and G.P. Peterson. Int. J. Heat Mass Transfer, **40**, 4329 (1997).
17. H. Branover. Magnetohydrodynamic flow in ducts. John Wiley & Sons, Inc., New York, N.Y. 1978.
18. F.G. Blottner. AIAA J. **8**, 193 (1970).

Appendix A: List of symbols

$B(x)$	magnetic induction, $B(x) = B_0(Mx + N)^{(n-1)/4}$
c_p	specific heat
C_f	skin-friction coefficient defined by (14a)
$f(\eta)$	similarity stream function
f_0	dimensionless wall mass transfer parameter, $f_0 = v_0 / \left[\frac{g^*\beta\Delta T\nu^2}{\lvert M\rvert^3}\right]^{1/4} M(\frac{n+3}{4})$
g^*	gravitational acceleration
$g(\eta)$	similarity temperature
Ha^2	square of the Hartmann number, $\mathrm{Ha}^2 = \sigma B_0^2 / \left[\rho(g^*\beta\Delta T\lvert M\rvert)^{1/2}\right]$
k	thermal conductivity
K^*	grid growth factor
m	parameter describing whether the environment temperature ($m = 0$) or the wall temperature ($m = -1$) is fixed
M	coefficient in the ξ coordinate
n	parameter describing the variation of the wall and environment temperature
N	coefficient in the ξ coordinate
Nu	Nusselt number defined by (14b)
p	pressure
Pr	Prandtl number
$Q(x)$	heat generation or absorption coefficient, $Q(x) = Q_0(Mx + N)^{(n-1)/2}$
T	temperature
T_c	constant temperature
$T_w(x)$	wall temperature, $T_w(x) = (m + 1)\Delta T\xi^n + T_c$
$T_\infty(x)$	environment temperature, $T_\infty(x) = m\Delta T\xi^n + T_c$
u	vertical velocity component
v	velocity component perpendicular to the plate
$v_w(x)$	wall mass transfer parameter, $v_w(x) = v_0(Mx + N)^{(n-1)/4}$
x	vertical coordinate
y	coordinate perpendicular to, and beginning at, the plate
α	dimensionless internal heat generation/absorption coefficient, $\alpha = \frac{Q_0}{\rho\, c_p(g^*\beta\Delta T\lvert M\rvert)^{1/2}}$
β	coefficient of thermal expansion
ΔT	characteristic temperature difference, $\Delta T = T_w - T_\infty(0)$
$\Delta\eta$	grid size in the η direction
η	similarity y-coordinate
μ	dynamic viscosity
ν	kinematic viscosity
ξ	transformed x-coordinate, $\xi = Mx + N$
ρ	density
σ	electrical conductivity
ψ	stream function

Superscript

$'$	differentiation with respect to η

Subscripts

w	wall condition
∞	environment condition